Bulletin of the Seismological Society of America, Vol. 93, No. 1, pp. 386–396, February 2003

Relationship between Peak Ground Acceleration, Peak Ground Velocity, and Intensity in Taiwan

by Yih-Min Wu, Ta-liang Teng, Tzay-Chyn Shin, and Nai-Chi Hsiao

Abstract Based on the strong-motion data set from the 1999 Chi-Chi, Taiwan, earthquake and a shaking damage statistics database, we investigated the correlations between strong ground motions and earthquake damage (fatalities and building collapses) through a regression analysis. As a result, the current earthquake intensity scale I_t is placed on a more reliable instrumental basis. This is necessary for the real-time seismic monitoring operation in Taiwan where programs for earthquake rapid reporting (RRS) and earthquake early warning (EWS) are actively pursued. It is found that the earthquake damage statistics give a much closer correlation with the peak ground velocity (PGV) than with the peak ground acceleration (PGA). The empirical relationship between PGV and the intensity I_t determined in this study can be expressed as

$$I_t = 2.14 \times \log_{10}(\mathrm{PGV}) + 1.89.$$

This PGV-based intensity is particularly useful in real-time applications for damage prediction and assessment, as the damage impact of high PGV is much more important for mid-rise and high-rise buildings that are characteristic of a modern society. For smaller earthquakes ($M < 5$), the PGV-intensity correlation also out-performs the PGA-intensity correlation, as large sharp PGA spikes are often observed for rather small nondamaging events at close-in distances. However, as the lower level intensity is conventionally defined through human feelings, for even smaller events ($M < 3$) humans are more sensitive to PGA than to PGV. Since the RRS and EWS operations are mainly dealing with large and damaging earthquakes, the above PGV-based empirical relationship should prove to be more appropriate in these real-time operations.

Introduction

Seismic intensity is a practical index describing, at a particular site, the degree of shaking or damage. An intensity map gives the shaking pattern reflected by the earthquake damage and effects on humans from an earthquake. In the absence of instrumental recordings, the intensity scale was originally designed to be descriptive and qualitative when it was first introduced more than a century ago in Europe and modified in later applications (Wood and Neumann, 1931; Richter, 1958). At lower levels of the scale, the intensity is generally assessed in terms of how the shaking is felt by people. Higher levels of the scale are based on observed structural damage surveyed by professionals.

Seismic intensity observation in Taiwan began in the 1930s. A seven-level intensity scale (0 to 6) was used until 2000. After the 1999 Chi-Chi earthquake, the intensity scale was extended to eight levels (0 to 7) due to the widespread pattern of high ground accelerations (400 Gal and greater), above which there was observed a rapid increase in fatality rate from 0.054% to 1.112% of the involved population (Tsai *et al.*, 2001). An additional intensity level 7, defined for PGA > 400 Gal, was required to address the severity of the ground motion and the consequent damage. The intensity scale of Taiwan is similar to that used in Japan, and a comparison with the Modified Mercalli intensity scale is given in Table 1.

Early comparisons of peak ground motions and intensities were based primarily on regressions of the intensity levels against the limited recorded PGA values (Trifunac and Brady, 1975; Hsu, 1979). Table 2 shows the current PGA-based intensity scale used in Taiwan. But the PGA-based intensity is often quite erratic in that for even small to moderate events there are occasionally large PGA values that are only confined to some small "singular" neighborhoods such as the case of Tarzana, California, during the 1994 Northridge earthquake. These singular values are largely due to highly variable local site effects and wave propagation ef-

Table 1
A Comparison of PGV-Based Intensity Scale I_t of Taiwan (This Study) and the PGV-Based Intensity Scale for California (Wald *et al.*, 1999)

CWB Intensities (This Study)									
Intensity	0	1	2	3	4	5	6	7	
PGA (Gal)	<0.8	0.8–2.5	2.5–8	8–25	25–80	80–250	250–400	>400	
PGV (cm/sec)	<0.22	0.22–0.65	0.65–1.9	1.9–5.7	5.7–17	17–49	49–75	>75	
Modified Mercalli Intensities (David *et al.*, 1999)									
Intensity	1	2–3	4	5	6	7	8	9	10
PGA (Gal)	<1.7	1.7–14	14–39	39–92	92–180	180–340	340–650	650–1240	>1240
PGV (cm/sec)	<0.1	0.1–1.1	1.1–3.4	3.4–8.1	8.1–16	16–31	31–60	60–116	>116

Table 2
Intensity Scale I_t Versus Peak Ground Acceleration (PGA) in Use in Taiwan

Intensity	PGA (Gal)	Perceived Shaking	Potential Damage
0	<0.8	Not felt	None
1	0.8–2.5	Very light	None
2	2.5–8	Light	None
3	8–25	Weak	None
4	25–80	Moderate	Very light
5	80–250	Strong	Light
6	250–400	Violent	Moderate
7	>400	Extreme	Heavy

fects, especially when the ground motions are dominated by high frequencies. This phenomenon has been observed often, as Taiwan installed a dense 650-station strong-motion instrument array (the TSMIP array, Fig. 1) in the 1990s, and this array has greatly increased the observed strong-motion database. To illustrate the different behaviors of PGA and PGV, we first give three examples showing that for large earthquakes among different sites, PGA values can have large variations, whereas corresponding PGV values give smaller variations. In Figure 2, three near-field records of large earthquakes are shown: (A) gives the record of an M 6.3 event with a sharp and narrow peak of PGA = 1113 Gal and PGV = 40 cm/sec; (B) and (C) give the record of the 1999 Chi-Chi earthquake of M 7.6 with moderately high values of PGA = 326 Gal and 179 Gal, and PGV = 289 cm/sec and 82 cm/sec, respectively. It is clear that for large earthquakes the PGA values vary in large ranges and do not reflect the actual earthquake magnitude as well as the PGV values. In Figure 3, we give three examples of ground-motion records for small earthquakes at close-in distances. All three cases show surprisingly high PGA values. In (A) an M 3.69 event yields a PGA value of 549 Gal, and PGV = 6.6 cm/sec; in (B) an M 4.7 event yields a PGA of 269 Gal, and PGV = 17.3 cm/sec; and in (C) an M 4.83 event yields a PGA of 501 Gal, and PGV = 21.6 cm/sec. Clearly, each of these large PGA values is characterized by a single sharp peak rich in high frequencies, and spatially the high values drop off quickly outside certain neighborhoods. The corresponding PGV values usually do not show these singular high values in space and time. As the strong-motion velocity signal integrates the acceleration signal, it averages and smooths out the large PGA amplitude variations.

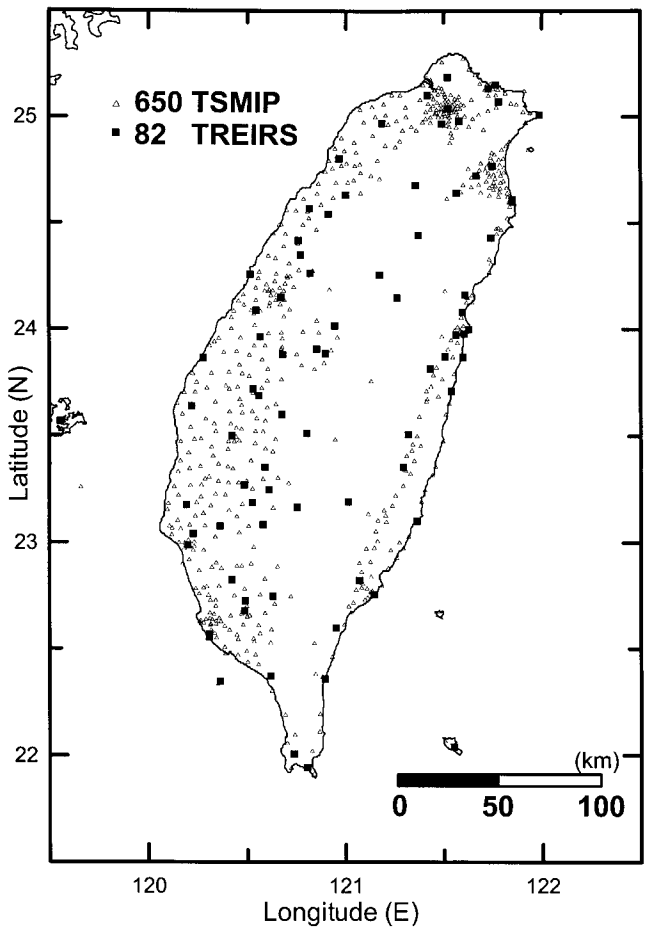

Figure 1. Free-field strong-motion stations in Taiwan: open triangles are the Taiwan Strong-Motion Instrumentation Program (TSMIP) 650 stations. Solid squares are 82-station telemetered strong-motion stations (TREIRS). Few stations are in the Central Mountain Range, which is sparsely populated.

The TSMIP has a station spacing of about 5 km in the

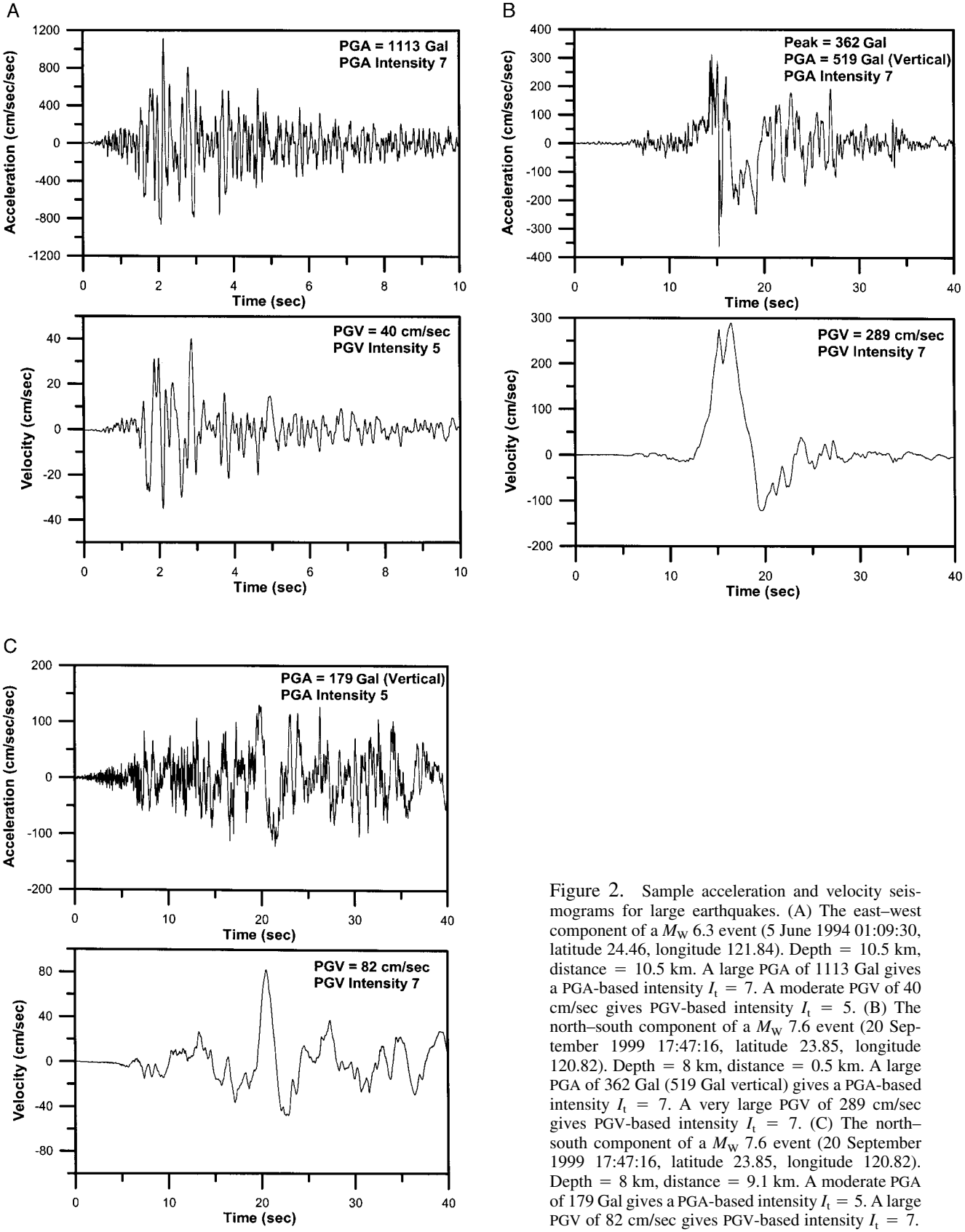

Figure 2. Sample acceleration and velocity seismograms for large earthquakes. (A) The east–west component of a M_W 6.3 event (5 June 1994 01:09:30, latitude 24.46, longitude 121.84). Depth = 10.5 km, distance = 10.5 km. A large PGA of 1113 Gal gives a PGA-based intensity I_t = 7. A moderate PGV of 40 cm/sec gives PGV-based intensity I_t = 5. (B) The north–south component of a M_W 7.6 event (20 September 1999 17:47:16, latitude 23.85, longitude 120.82). Depth = 8 km, distance = 0.5 km. A large PGA of 362 Gal (519 Gal vertical) gives a PGA-based intensity I_t = 7. A very large PGV of 289 cm/sec gives PGV-based intensity I_t = 7. (C) The north–south component of a M_W 7.6 event (20 September 1999 17:47:16, latitude 23.85, longitude 120.82). Depth = 8 km, distance = 9.1 km. A moderate PGA of 179 Gal gives a PGA-based intensity I_t = 5. A large PGV of 82 cm/sec gives PGV-based intensity I_t = 7.

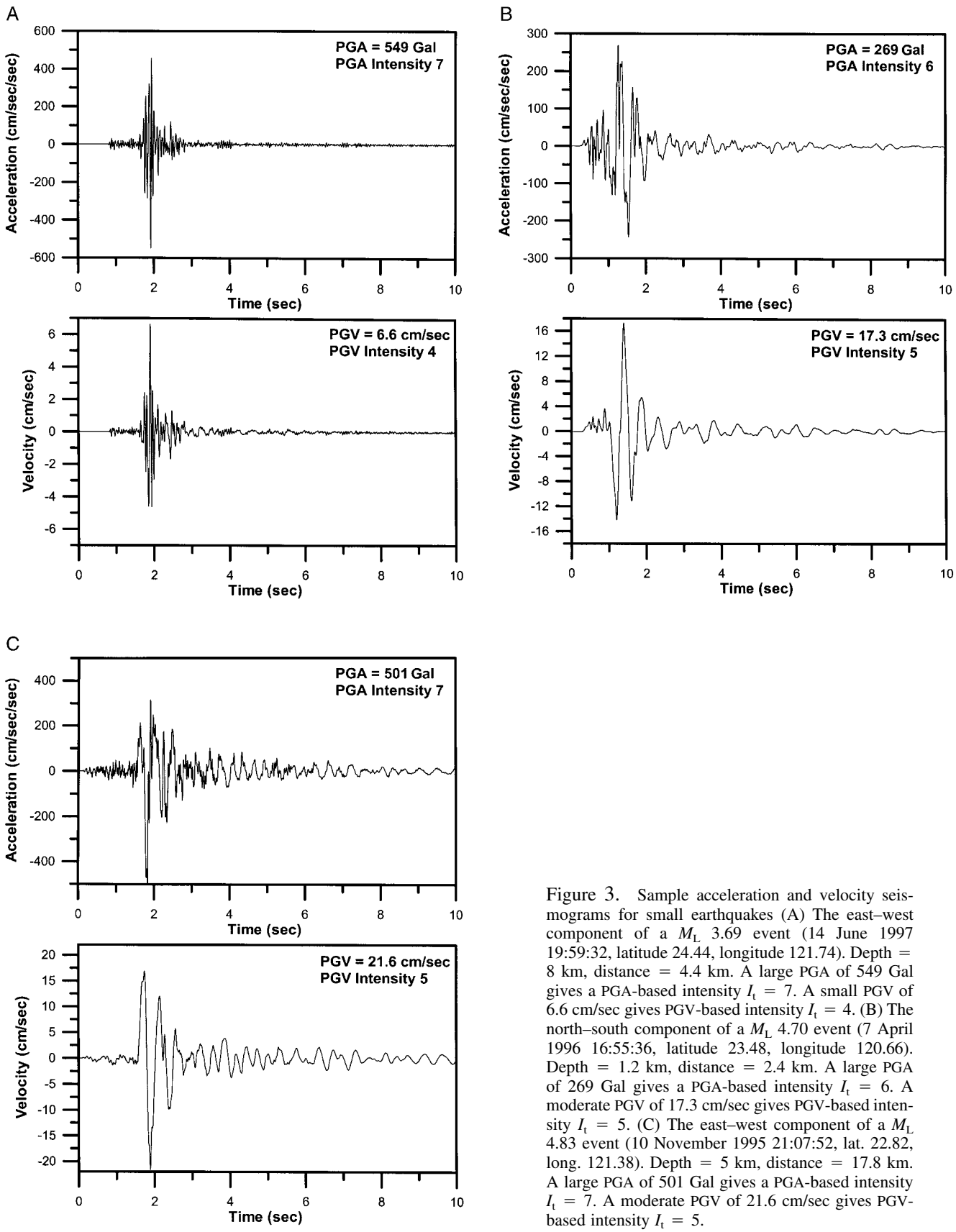

Figure 3. Sample acceleration and velocity seismograms for small earthquakes (A) The east–west component of a M_L 3.69 event (14 June 1997 19:59:32, latitude 24.44, longitude 121.74). Depth = 8 km, distance = 4.4 km. A large PGA of 549 Gal gives a PGA-based intensity I_t = 7. A small PGV of 6.6 cm/sec gives PGV-based intensity I_t = 4. (B) The north–south component of a M_L 4.70 event (7 April 1996 16:55:36, latitude 23.48, longitude 120.66). Depth = 1.2 km, distance = 2.4 km. A large PGA of 269 Gal gives a PGA-based intensity I_t = 6. A moderate PGV of 17.3 cm/sec gives PGV-based intensity I_t = 5. (C) The east–west component of a M_L 4.83 event (10 November 1995 21:07:52, lat. 22.82, long. 121.38). Depth = 5 km, distance = 17.8 km. A large PGA of 501 Gal gives a PGA-based intensity I_t = 7. A moderate PGV of 21.6 cm/sec gives PGV-based intensity I_t = 5.

populated area of Taiwan (Fig. 1). It gives strong-motion recordings of high spatial resolution, and it is commonly noted that occasionally large PGA values for small events usually occur in small local singular neighborhoods and the high PGA peaks disappear quickly when removed from these locations. We have assembled a set of 2036 TSMIP measurements of PGA values that are larger than 80 Gal. When the PGA values and the corresponding PGV values are plotted against local magnitude M_L, with the current intensity scale I_t plotted along the right-hand side, we find that the PGA values do not have the resolution to distinguish large from small events. Figure 4A is a plot of all data with PGA $>$ 80 Gal. Events as small as $M_L \sim 3.5$ can generate a PGA $>$ 500 gal that would give rise to an intensity $I_t = 7$. The data show that PGA alone has difficulty to discriminate the magnitude and intensity. However, in Figure 4B, the PGV values are more discriminative, as the maximum PGV values are more proportional to M_L and give rise to more reasonable intensity levels. To calculate a new JMA instrument-based intensity scale, a low-pass filter is applied to the recorded acceleration and the shaking duration is also considered (Sekita, 1996). Recent work in California shows that for instrumental data and intensity values of eight California earthquakes (from 1971 San Fernando to 1992 Landers), a closer correlation is found between PGV and the intensity than between PGA and intensity (Wald *et al.*, 1999). Since the Chi-Chi earthquake is a well-recorded large event that has generated an extensive data set for strong motions and a well-document damage and casualty statistics, we shall use these two data sets to derive a PGV-based intensity scale for Taiwan.

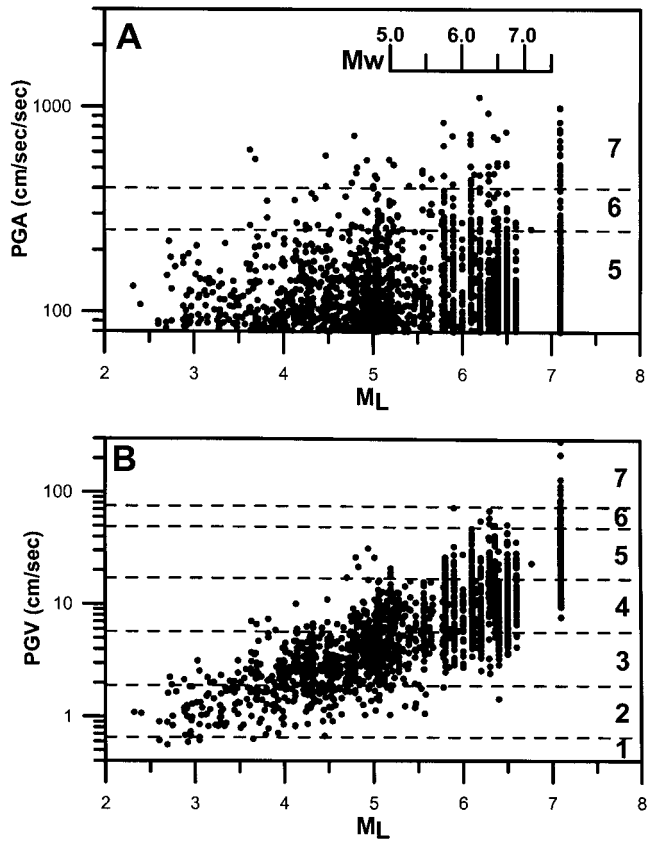

Figure 4. (A) A plot of 2036 records of PGA $>$ 80 Gal vs. M_L. The PGA-based intensity scale I_t is plotted along the right-hand side. The PGA data show a lack of resolution in intensity determination. (B) A corresponding plot of PGV values versus M_L. The PGA-based intensity scale I_t is plotted along the right-hand side. The PGV data show a much-improved resolution in intensity determination. Note: For a given event, the PGA and PGV occupy a range of intensity due to change of epicentral distance.

Data and Damage Statistics

Data used in this analysis come from two sources. Both data sets are large and are perhaps as complete as those obtained from any earthquake in the world so far.

Strong-Motion Data

The Taiwan Strong-Motion Instrumentation Program (TSMIP) was successfully implemented in the early 1990s with a total of 650 modern digital accelerographs deployed at free-field sites (triangles in Fig. 1). Adding to the TSMIP stations are another 82 telemetered digital accelerographs (squares in Fig. 1). Except in the unpopulated Central Mountain Ranges that form the high-relief backbone of Taiwan, the TSMIP gives a regional deployment of modern accelerographs with an average station spacing of about 5 km. During the 1999 Chi-Chi, Taiwan, earthquake, 441 of these strong-motion instruments wrote excellent records, thoroughly describing the acceleration field generated by the mainshock. Data from this mainshock were used in our regression analysis. These accelerographs are equipped with broadband force-balanced sensors (FBAs) with response essentially flat from DC to 50 Hz. Recording is done at 200 sample/sec with 16-bit resolution and 2g dynamic range. Integration of the FBA acceleration signals to velocity and displacement can be done accurately, as described in a number of recent articles (Iwan *et al.*, 1985; Boore, 2001). Accurate measurements of both PGA and PGV can thus be made from these recordings.

Damage Statistics

The government of Taiwan has perhaps the most thorough, detailed demographic data and information on the dwelling types and locations of its citizens in the world. During the aftermath of the Chi-Chi earthquake, a massive mobilization of professional people, particularly civil and structural engineers, as well as medical practitioners, was called to survey the meizoseismic area where detailed damage and human losses were carefully documented and statistics archived (National Office of Statistics, 2001). Here, we would use the term "household" as a damage unit instead of a house or a building. Earthquake damage in modern urban areas is quite different compared with the damage in

days when the MMI scale was first introduced. Single residential buildings are no longer the norm of a modern heavily populated urban area. Mid-rise and high-rise structures that come in all shapes and sizes dominate urban areas, and each structure may house tens to hundreds of household units. Therefore, damage statistics can be more accurately described by the number of households than by the number of structures. We may consider the term "household" here as referring to an equivalent single dwelling unit. Also, the number of households provides a clear link to the total affected population involved if the number of persons per household can be determined statistically. In all, during the 1999 Chi-Chi earthquake, there were 51,753 totally collapsed households, 54,406 partially collapsed households, 2,489 dead, and 11,306 injured (of which 725 were seriously injured). Volumes of tabulations are kept not only as a historical record, but also more importantly as the basis for postearthquake reconstruction and rehabilitation. We have extracted the statistical data to form one input of our regression analysis from which we have derived an intensity scale that quantitatively describes the data. Figure 5 shows the distribution of townships and their boundaries over Taiwan. The township is a useful geographical unit for our analysis because it is the basic bin according to which the National Office of Statistics categorizes damage data. The large Chelungpu rupture and the epicenter of the 1999 Chi-Chi earthquake are also plotted in Figure 5. Regions of particularly dense population are enlarged to show that for an island of 36,000 km^2 with 23 million people, the township subdivisions can be quite fine and earthquake damage statistics can be quite thoroughly mapped on the basis of a detailed household registration database. Note also that in Figure 5, a solid square is placed at the geometric center of each township, and we have arbitrarily assigned the damage statistics with this township point. We have enlarged regions of high population (Taipei in the north and Kaohsiung in the south), as well as the Taichung region surrounding the Chelungpu rupture, where heavy damage and a large number of casualties occurred. For example, Figure 6 shows a plot of the PGA contours versus the percentage rate of household collapse, and Figure 7 shows the PGV contours versus the percentage rate of fatality. In both figures, we superpose over the base map township boundaries and the Chelungpu fault trace. The Taipei metropolitan area is enlarged as an insert at the lower right of Figures 6 and 7. It is seen that upon integration, some of the sharp PGA peaks in Figure 6 (dark spots around the Chi-Chi epicenter) are averaged and smoothed out to form broader and milder high-value areas in the corresponding PGV plot (Fig. 7).

Correlation Analysis

For regression analysis, we first averaged the township damage and fatality rates in different PGA and PGV value ranges, and then these average values were used as inputs into the regression analysis. This averaging accomplished a degree of local smoothing that avoids singular sites of unusual responses; it also avoided points of zero data when logarithms of the values were taken. Results of the regression analysis are given in Figure 8 for PGA and Figure 9 for PGV. Each of these two figures has three parts: (A) for percentage fatality rate, (B) for percentage household total collapse rate, and (C) for percentage household partial collapse rate. In part A of Figure 8, the anomalous data point labeled Taipei Basin refers to a location 150 km away from the Chi-Chi epicenter, where the PGA had attenuated to about 85 Gal but the PGV remained relatively high (25 cm/sec) and lasted for a long duration; this had brought down a few high-rise buildings that accounted for the high fatality rate. In both parts B and C, there is an anomalously low point lying in the range of 600–700 Gal. This point may be explained by the presence of several events that occurred near the two ends of the Chelungpu fault within 1 min after the mainshock (Shin, 2000). These events caused high-frequency acceleration signals to mix in with the mainshock arrivals, thus producing high PGA. However, this mixing of signals did not cause a higher PGV value or significant damage. The PGV correlations in Figure 9 give much tighter fits with smaller standard errors, whereas the PGA correlations in Figure 8 have a number of disparate data points that reflect the erratic nature of PGA, which often varies due to local site response irregularities. Therefore, for intensity calculation and damage assessment, a PGV-based empirical relationship is a more reasonable choice.

PGV Versus Intensity

The Central Weather Bureau of Taiwan has in the past derived an empirical relationship between PGA and intensity I_t as follows (Hsu, 1979; Wu *et al.*, 2002):

$$I_t = 2 \times \log_{10}(\mathrm{PGA}) + 0.7. \quad (1)$$

Here PGA is in Gal, and I_t is the calculated intensity after rounding off to the nearest integer. For PGA $>$ 400 Gal, it is defined that $I_t = 7$. Table 2 gives the currently used PGA-based intensity I_t. With the extensive strong-motion data and damage statistics available after the Chi-Chi event, we can proceed to obtain an empirical relationship between PGV and I_t. From a regression analysis, we have for the PGA:

$$\log_{10}(Fr) = -12.572 + 4.282 \times \log_{10}(\mathrm{PGA}) \quad (2)$$

$$\log_{10}(Ct) = -10.118 + 4.146 \times \log_{10}(\mathrm{PGA}) \quad (3)$$

$$\log_{10}(Cp) = -9.941 + 4.061 \times \log_{10}(\mathrm{PGA}) \quad (4)$$

and for the PGV:

$$\log_{10}(Fr) = -9.360 + 4.315 \times \log_{10}(\mathrm{PGV}) \quad (5)$$

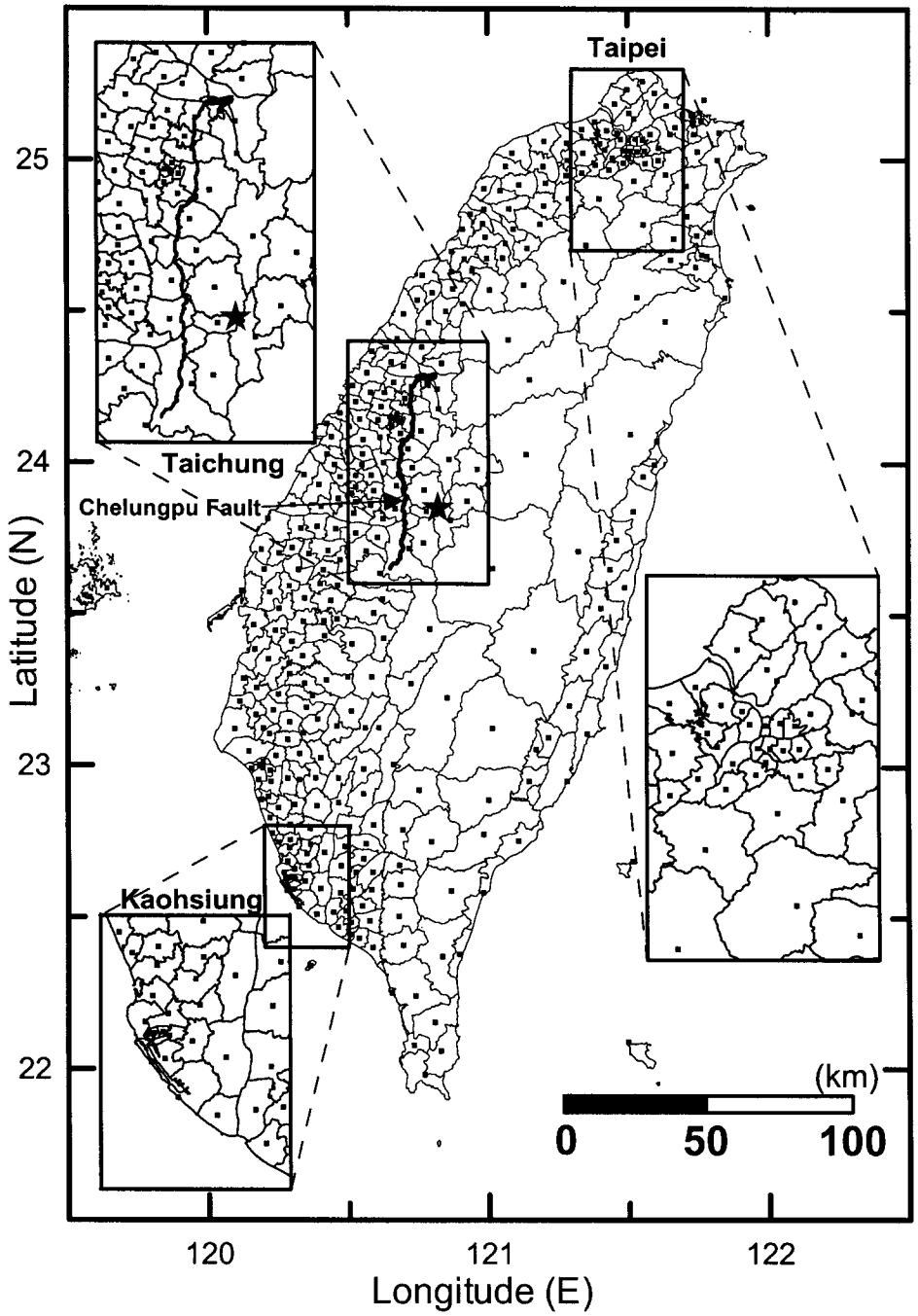

Figure 5. A map of Taiwan marking the boundaries of townships, which is the basis of household registration. In regions of high population (Taipei in the north and Kaohsiung in the south), enlarged inserts are shown. Also shown are the Chelungpu fault (the causal fault of the 1999 Chi-Chi, Taiwan, earthquake), and the Chi-Chi mainshock epicenter. The Taichung mezoseismic region is also shown enlarged.

$$\log_{10}(Ct) = -8.452 + 4.825 \times \log_{10}(\mathrm{PGV}) \quad (6)$$

$$\log_{10}(Cp) = -8.007 + 4.452 \times \log_{10}(\mathrm{PGV}). \quad (7)$$

Here, Fr, Ct, and Cp are the percentage rates of the fatality, totally collapsed households, and partially collapsed households, respectively. (Again, a household is an officially registered equivalent single dwelling unit). On the average, about 3.3 people occupy a household in the Taiwan area. Substituting equations (2), (3), and (4) into equations (5), (6), and (7), we eliminate the variables Fr, Ct, and Cp and derive three relationships between PGA and PGV, as follows:

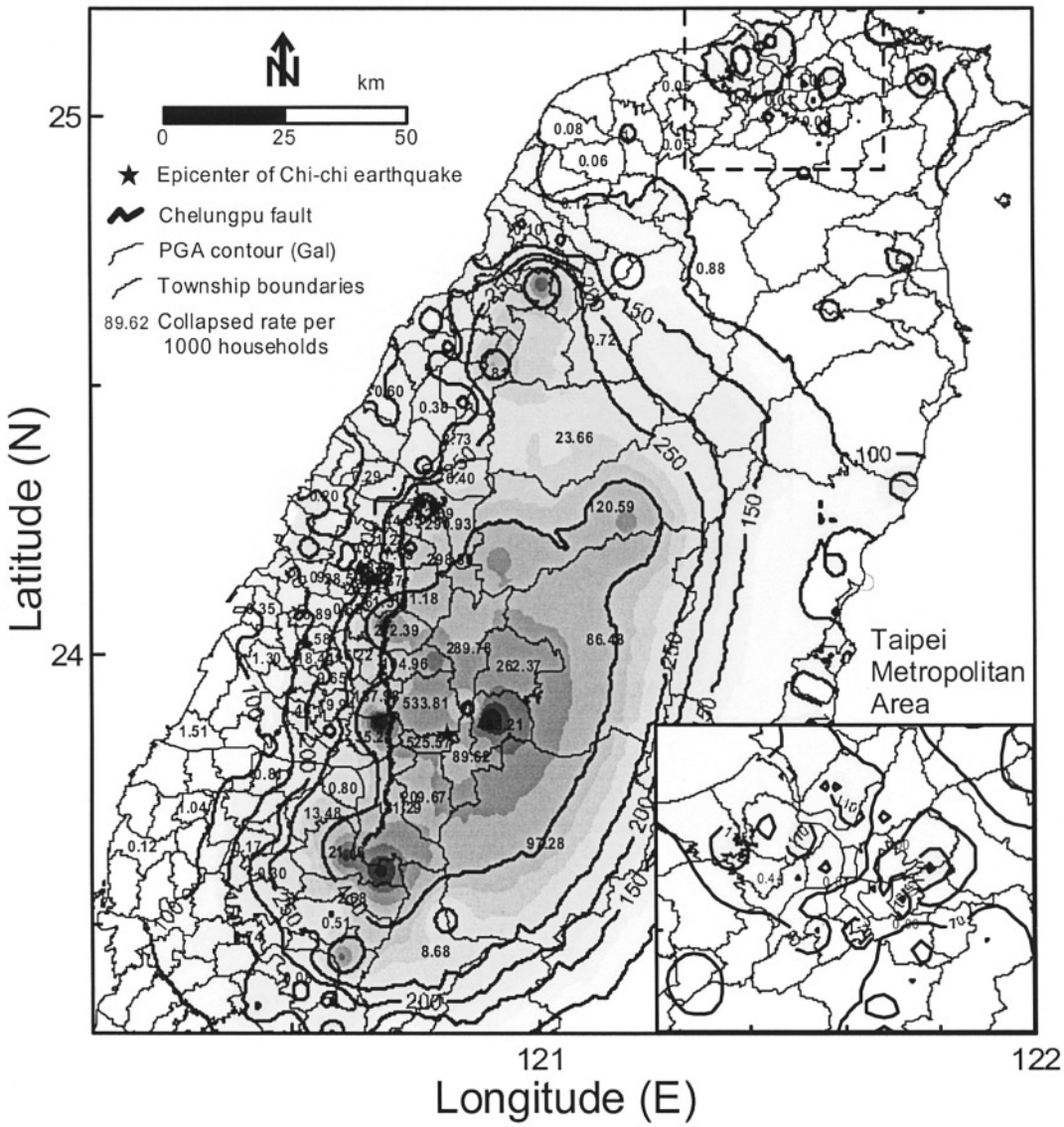

Figure 6. A PGA contour plot of central and north Taiwan showing the damage figures (collapse rate per 1000 households) on a township base map. Also shown are the Chelungpu fault (the causal fault of the 1999 Chi-Chi, Taiwan, earthquake), and the Chi-Chi mainshock epicenter. An enlarged portion of the Taipei metropolitan area is given at the lower right.

$$\log_{10}(\mathrm{PGA}) = 0.750 + 1.008 \times \log_{10}(\mathrm{PGV}) \quad (8)$$

$$\log_{10}(\mathrm{PGA}) = 0.402 + 1.164 \times \log_{10}(\mathrm{PGV}) \quad (9)$$

$$\log_{10}(\mathrm{PGA}) = 0.476 + 1.096 \times \log_{10}(\mathrm{PGV}) \quad (10)$$

Equations (8), (9), and (10) are determined from, and therefore carry the information of, percentage rates of the fatality, totally collapsed households, and partially collapsed households, respectively. We first take the average of equations (9) and (10), as they come from the building damage category. It gives

$$\log_{10}(\mathrm{PGA}) = 0.439 + 1.130 \times \log_{10}(\mathrm{PGV}) \quad (11)$$

Then we take into account the fatality contribution by averaging equations (8) and (11). The final empirical relationship between PGA and PGV is:

$$\log_{10}(\mathrm{PGA}) = 0.595 + 1.069 \times \log_{10}(\mathrm{PGV}) \quad (12)$$

Substituting equation (12) into equation (1), we have a relationship between PGV and the intensity I_t as follows:

$$I_t = 2.14 \times \log_{10}(\mathrm{PGV}) + 1.89. \quad (13)$$

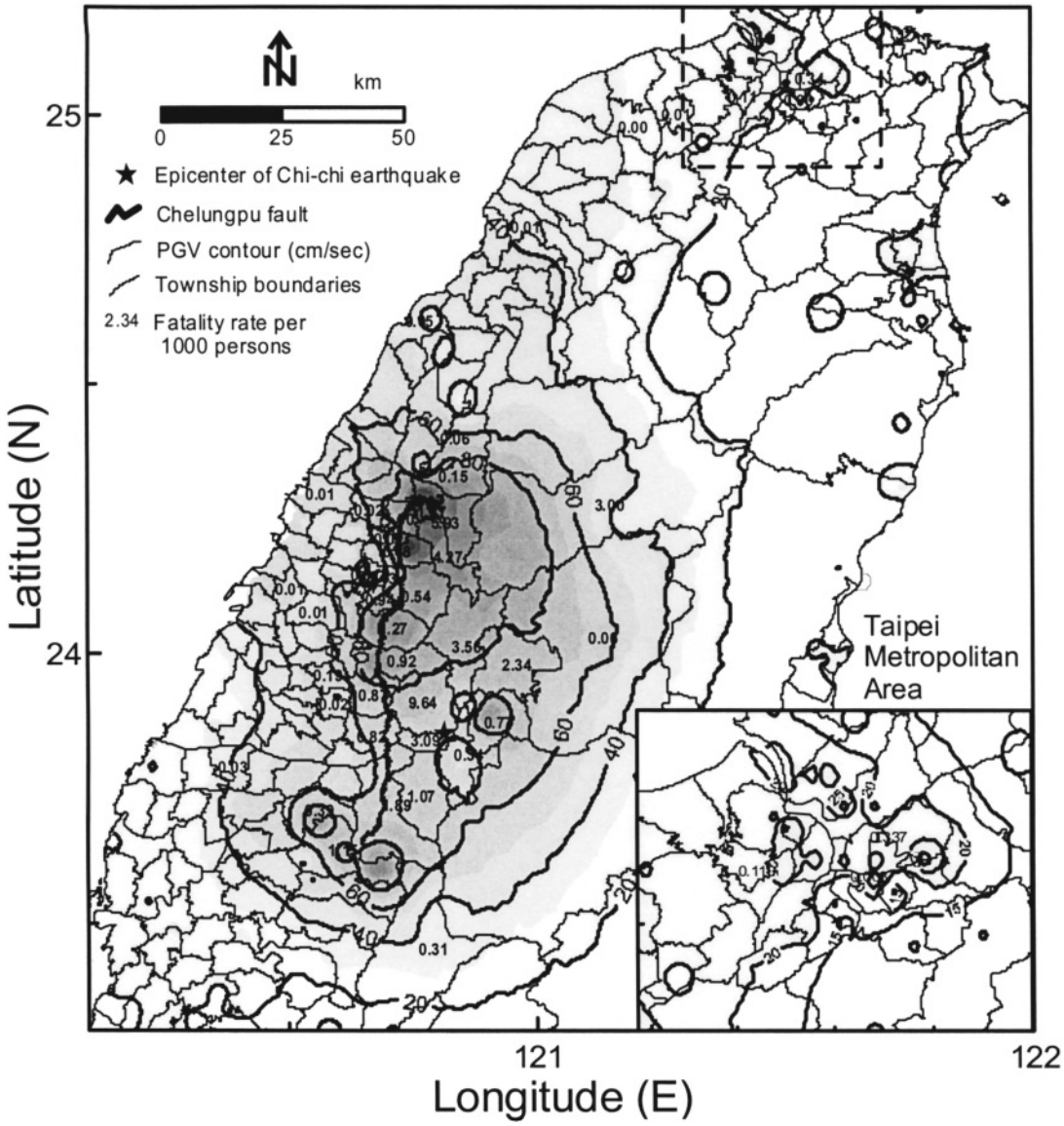

Figure 7. A PGV contour plot of central and north Taiwan showing the casualty figures (fatality rate per 1000 people) on a township base map. Also shown are the Chelungpu fault (the causal fault of the 1999 Chi-Chi, Taiwan, earthquake), and the Chi-Chi mainshock epicenter. An enlarged portion of the Taipei metropolitan area is given at the lower right.

Here PGV is in cm/sec, and I_t is the PGV-based intensity, rounding off to the nearest integer. We also define that for PGV $>$ 75 cm/sec, $I_t = 7$. The top three rows of Table 1 show the PGV-based intensity I_t derived in this study. The corresponding PGA values are also given. The bottom three rows of Table 1 offer a comparison with the MMI intensity scale derived by Wald *et al.* (1999) for California, with corresponding PGA and PGV ranges. This newly derived PGV-based I_t gives an empirical link to the potential earthquake damage in terms of percentage rates of the fatality, totally collapsed households, and partially collapsed households. For large earthquakes, this link is useful especially in emergency response, disaster management, and earthquake loss assessment.

Discussions and Conclusions

Seismic monitoring in Taiwan has been conducted for nearly a century, and reporting earthquake intensity using a scale akin to the Japanese JMA intensity scale has been done for more that 70 years. Past observations show that almost never has there been any earthquake damage caused by events of M_L less than 5. However, it is not uncommon that even for small ($M_L \sim 4$) events, PGA values may reach above

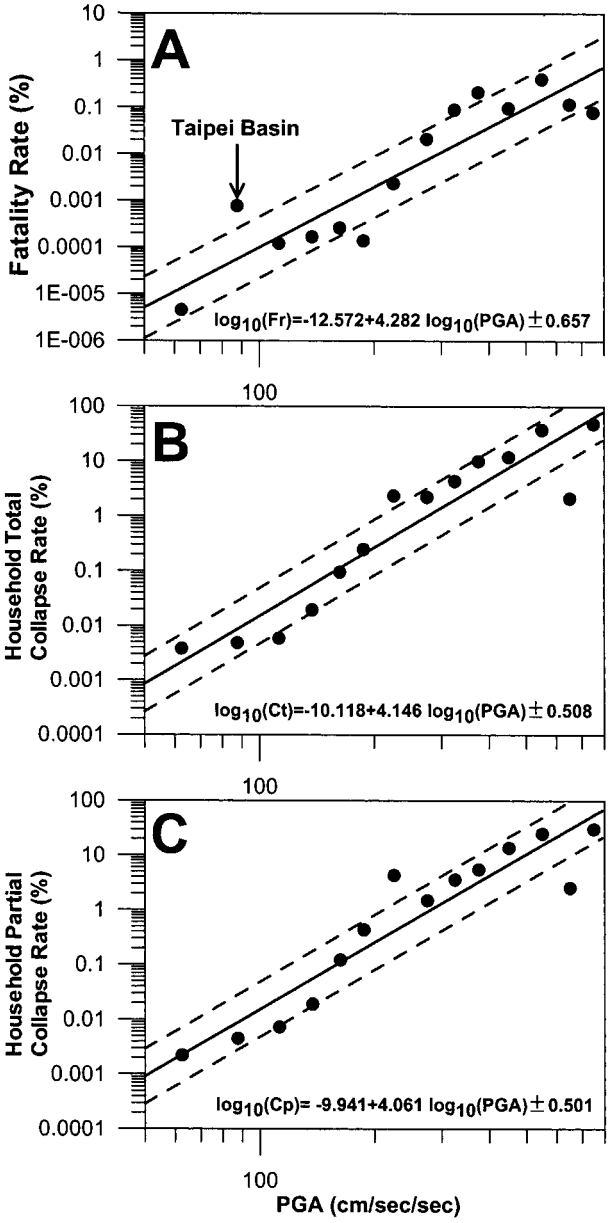

Figure 8. Results of the regression analysis giving the correlation between PGA values and (A) the fatality rate, (B) household total collapse rate, and (C) household partial collapse rate. Dashed lines give one standard deviation. Each data point represents a range of PGA in which the rates are averaged. In (A), the data point labeled Taipei Basin comes from the collapse of several high-rise residential building 150 km away in Taipei basin, resulting in many deaths. Also, in all three plots, the standard errors are large with a considerable number of outlying data points.

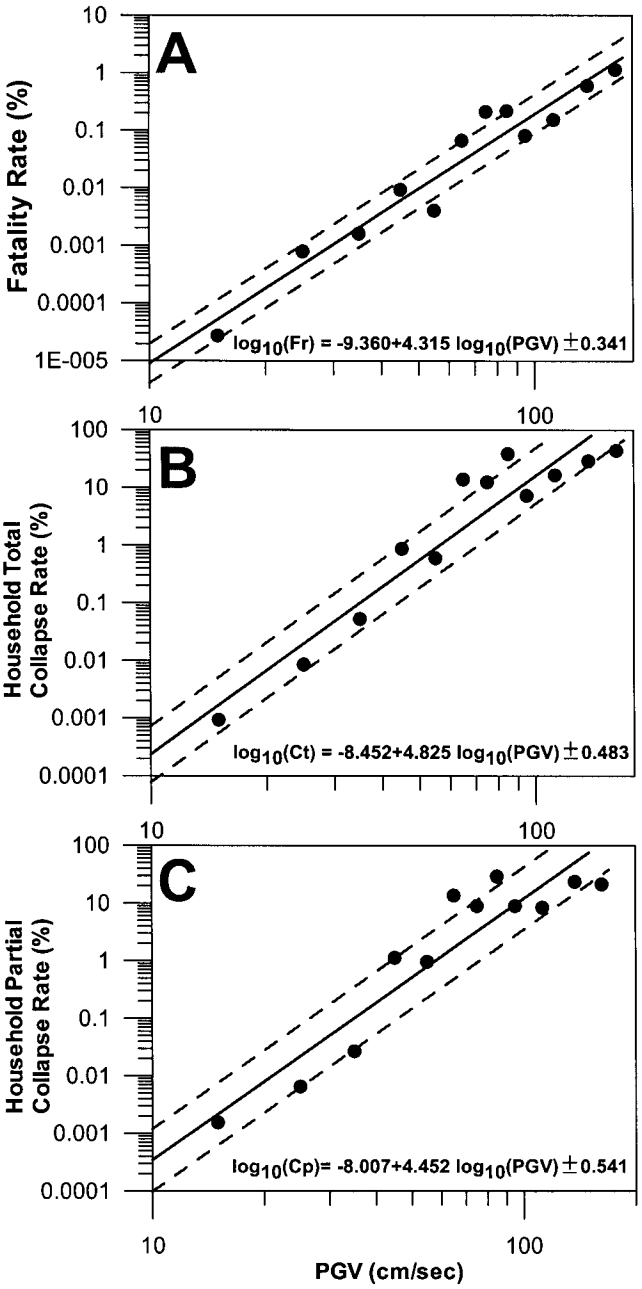

Figure 9. Results of the regression analysis giving the correlation between PGV values and (A) the fatality rate, (B) household total collapse rate, and (C) household partial collapse rate. Dashed lines give one standard deviation. Each data point represents a range of PGV in which the rates are averaged. All three plots show reduced standard errors with far less disparate data points than the PGA plots in Figure 8.

500 Gal. These PGA peaks are usually sharp, impulselike, and rich in high-frequency content. When intensity is determined from these PGA values, it produces intensity estimates larger than 4, and even as large as 7—a phenomenon long considered to be unreasonable. In this study, we take advantage of the two large data sets and directly tie the PGV measurements to the damage statistics. Through a regression analysis, we show that earthquake damage correlates much better with PGV values than with PGA values. Through the correlation results, we derive an empirical relationship that allows intensity to be more quantitatively evaluated using data form the strong-motion array established in Taiwan.

Our results compare favorably with those from the JMA approach in Japan based on PGV (Sekita, 1996) and from a similar PGV-based approach in California (Wald *et al.*, 1999). In recent years, the Taiwan Central Weather Bureau (CWB) has engaged in the development of an earthquake rapid reporting system (RRS) and an earthquake early warning system (EWS). The development is based on an 82-station network of real-time telemetered strong-motion accelerographs. In RRS, CWB has reached the goal of issuing earthquake reports within one minute of the event occurrence (Teng *et al.*, 1997; Wu *et al.*, 1997, 2000, 2001). For EWS, a recent article (Wu and Teng, 2002) reported that for some cases, an early warning can be issued up to 20 sec before the strong shaking arrivals. What is needed for both RRS and EWS at this point is the ability to compute in near real-time for an event a more quantitative and reasonable intensity and damage/fatality prediction, which can be issued in parallel with the hypocenter and magnitude as part of the RRS and EWS operations. Since the output of the real-time strong-motion network is FBA signals for the accelerations, direct online numerical integration can determine the velocity, from which PGV values are readily computed. Therefore, using equations (5), (6), (7), and (13) from this study, the intensity I_t can be readily obtained together with damage/fatality prediction for emergency response purposes. With the 82-station telemetered strong-motion network, a rough intensity map can be constructed and delivered together with the RRS and/or EWS reports. For archiving purposes, of course, the finalized intensity map, determined offline, will make use of the complete output of the 650-station TSMIP free-field strong-motion array. Of course, new damage/fatality statistics will be compiled after each disastrous event to calibrate the present predictive ability.

Acknowledgments

We thank the two reviewers for their comments and suggestions that have significantly improved the manuscript. This study was supported by the Central Weather Bureau and the National Science Council of the Republic of China under Grant Number NSC90-2625-Z-052-009. T.L.T. was supported by Contract Number MTOC-CWB-90-E-05 and NSF EAR-00010616.

References

Boore, D. (2001). Effect of baseline corrections on displacements and response spectra for several recordings of the 1999 Chi-Chi, Taiwan earthquake, *Bull. Seism. Soc. Am.* **91,** 1191–1211.

Hsu, M. T. (1979). *Seismology*, Lee-Ming Culture Publication Company, Taipei, Taiwan, 16–26 (in Chinese).

Iwan, W. D., M. A. Mozer, and C.-Y. Peng (1985). Some observations on strong-motion earthquake measurement using a digital accelerograph, *Bull. Seism. Soc. Am.* **75,** 1225–1246.

National Office of Statistics (2001). Important statistics about the Chi-Chi earthquake disaster, 921 Earthquake Post-Disaster Recovery Commission, http:/www.921erc.gov.tw (in Chinese).

Richter, C. F., (1958) *Elementary Seismology*, W.H. Freeman and Company, San Francisco, 135–149, 650–653.

Sekita, Y. (1996). About the new JMA intensity scale (in Japanese), *JSEEP News* **147,** 21–26.

Shin, T. C., (2000). Some seismological aspects of the 1999 Chi-Chi earthquake in Taiwan. *TAO* **11,** 555–566.

Teng, T. L., Y. M. Wu, T. C. Shin, Y. B. Tsai and W. H. K. Lee (1997). One minute after: strong-motion map, effective epicenter, and effective magnitude, *Bull. Seism. Soc. Am.* **87,** 1209–1219.

Tsai, Y. B., T. M. Yu, H. L. Chao, and C. P. Lee (2001). Spatial distribution and age dependence of human-fatality rates from the Chi-Chi, Taiwan, Earthquake of 21 September 1999, *Bull. Seism. Soc. Am.* **91,** 1298–1309.

Trifunac, M. D., and A. G. Brady (1975). On the correlation of seismic intensity scales with the peaks of recorded ground motion, *Bull. Seism. Soc. Am.* **65,** 139–162.

Wald, D. J., V. Quitoriano, T. H. Heaton, H. Kanamori (1999). *Earthquake Spectra* **15,** 557–564.

Wood, H. O., and F. Neumann (1931). Modified Mercalli intensity scale of 1931, *Bull. Seism. Soc. Am.* **21,** 277–283.

Wu, Y. M. and T. L. Teng (2002). A VSN approach to earthquake early warning, *Bull. Seism. Soc. Am.* **92,** no. 5, 2008–2018.

Wu, Y. M., C. C. Chen, T. C. Shin, Y. B. Tsai, W. H. K. Lee, and T. L. Teng (1997). Taiwan Rapid Earthquake Information Release System, *Seism. Res. Lett.* **68,** 931–943.

Wu, Y. M., N. C. Hsiao, T. L. Teng, and T. C. Shin (2002). Near real-time seismic damage assessment of the rapid reporting system, *TAO* **13,** 313–324.

Wu, Y. M., W. H. K. Lee, C. C. Chen, T. C. Shin, T. L. Teng, and Y. B. Tsai (2000). Performance of the Taiwan Rapid Earthquake Information Release System (RTD) during the 1999 Chi-Chi (Taiwan) earthquake, *Seism. Res. Lett.* **71,** 338–343.

Wu, Y. M., T. C. Shin, and C. H. Chang (2001). Near real-time mapping of peak ground acceleration and peak ground velocity following a strong earthquake, *Bull. Seism. Soc. Am.* **91,** 1218–1228.

Central Weather Bureau
Taipei, Taiwan, ROC
(Y.-M.W., T.-C.S., N.-C.H.)

Southern California Earthquake Center
University of Southern California
Los Angeles, California
(T.-L.T.)

Manuscript received 2 April 2002.